Environ Sci Pollut Res (2016) 23:11611–11619
DOI 10.1007/s11356-016-6358-1

RESEARCH ARTICLE

Effect of alginate on the aggregation kinetics of copper oxide nanoparticles (CuO NPs): bridging interaction and hetero-aggregation induced by Ca^{2+}

Lingzhan Miao[1,2] · Chao Wang[1,2] · Jun Hou[1,2] · Peifang Wang[1,2] · Yanhui Ao[1,2] · Yi Li[1,2] · Bowen Lv[1,2] · Yangyang Yang[1,2] · Guoxiang You[1,2] · Yi Xu[1,2]

Received: 2 November 2015 / Accepted: 25 February 2016 / Published online: 2 March 2016

Abstract The stability of CuO nanoparticles (NPs) is expected to play a key role in the environmental risk assessment of nanotoxicity in aquatic systems. In this study, the effect of alginate (model polysaccharides) on the stability of CuO NPs in various environmentally relevant ionic strength conditions was investigated by using time-resolved dynamic light scattering. Significant aggregation of CuO NPs was observed in the presence of both monovalent and divalent cations. The critical coagulation concentrations (CCC) were 54.5 and 2.9 mM for $NaNO_3$ and $Ca(NO_3)_2$, respectively. The presence of alginate slowed nano-CuO aggregation rates over the entire $NaNO_3$ concentration range due to the combined electrostatic and steric effect. High concentrations of Ca^{2+} (>6 mM) resulted in stronger adsorption of alginate onto CuO NPs; however, enhanced aggregation of CuO NPs occurred simultaneously under the same conditions. Spectroscopic analysis revealed that the bridging interaction of alginate with Ca^{2+} might be an important mechanism for the enhanced aggregation. Furthermore, significant coagulation of the alginate molecules was observed in solutions of high Ca^{2+} concentrations, indicating a hetero-aggregation mechanism between the alginate-covered CuO NPs and the unabsorbed alginate. These results suggested a different aggregation mechanism of NPs might co-exist in aqueous systems enriched with natural organic matter, which should be taken into consideration in future studies.

Keywords CuO nanoparticles · Aggregation kinetics · Alginate · Divalent electrolytes · Bridging interaction · Hetero-aggregation mechanism

Responsible editor: Thomas D. Bucheli

Electronic supplementary material The online version of this article (doi:10.1007/s11356-016-6358-1) contains supplementary material, which is available to authorized users.

✉ Jun Hou
hhuhjyhj@126.com

✉ Peifang Wang
pfwang2005@hhu.edu.cn

[1] Key Laboratory of Integrated Regulation and Resources Development on Shallow Lakes, Ministry of Education, Hohai University, Nanjing 210098, People's Republic of China

[2] College of Environment, Hohai University, 1 Xikang Road, Nanjing 210098, People's Republic of China

Introduction

Copper oxide nanoparticles (CuO NPs) have been widely used in a variety of industrial products such as anti-bactericide coatings, biomedicines, and toothpastes (Applerot et al. 2012; Zhou et al. 2006). Due to the large quantities produced and their widespread application, engineered nanoparticles will be inevitably released into aqueous environment (Nowack and Bucheli 2007). It has been demonstrated that CuO NPs have an acute toxic effect on bacteria (Karlsson et al. 2008; Zhao et al. 2013), decrease cell viability of activated sludge (Hou et al. 2015; Zhou et al. 2015), and cause oxidative stress in microalgae (Aruoja et al. 2009). According to recent studies, once released into aquatic environments, nanoparticles may interact with naturally occurring water components, which consequently may affect the potential toxicity and fate of nanoparticles in the environment (Burkart et al. 2015; Grillo et al. 2015; Nowack et al. 2012).

Stability of these highly reactive materials in aquatic environment is an essential parameter to evaluate their fate,

bioavailability, and potential toxic effects towards living organisms (Aiken et al. 2011; Miao et al. 2014; Philippe and Schaumann 2014). Existing scientific evidence suggested that a wide range of environmental factors, such as the particle properties (size, surface charge, morphology) and water chemistry (pH, ionic strength, redox conditions, natural organic matter (NOM)) will inevitably interact with CuO NPs and influence their physicochemical properties (aggregation, sedimentation, and dissolution) (Aiken et al. 2011; Chang et al. 2012; Nowack et al. 2012; Yang et al. 2013). It has been demonstrated that the solution pH can influence the surface charge through a pH-dependent protonation and deprotonation of surface hydroxyl groups (Philippe and Schaumann 2014), which affects the aggregation and transport of NPs. Effects of various electrolytes were also investigated, and divalent ions can promote agglomeration of NPs due to compression of the electrical double layer (Son et al. 2015). Typically, higher NOM concentrations result in enhanced NP stability (Adeleye et al. 2014; Grillo et al. 2015): more adsorbed mass of NOM on the NPs induces electrostatic repulsion (attributable to negatively charged carboxylate groups) and electrosteric repulsion for high molecular weight components (Philippe and Schaumann 2014; Zhang et al. 2009).

In addition to humic substances, a non-humic aquagenic (i.e., produced in the water column) fraction also accounts for an important fraction of NOM in natural environments. A representative non-humic fraction NOM is polysaccharides, which are widespread in aquatic systems and make up 10–30 % of the NOM in lakes (Chen et al. 2006; Wilkinson et al. 1997). Given the presence of both nanoparticles and polysaccharides in the environment, it is important to understand how they interact with each other and how those interactions may affect the transport and fate of NPs. Although some studies have demonstrated that polysaccharides can destabilize nanoparticle aggregates (Chen et al. 2006; Loosli et al. 2015), their role in influencing the aggregation kinetics of nanoparticles in complex water conditions is still not well understood. Furthermore, polysaccharide molecules can interact with themselves, leading to the formation of molecular aggregates dependent on the environmental conditions. In the presence of multivalent cations, Ca^{2+} for example, aggregation of polysaccharides is induced by charge neutralization and cation bridge formation between different polysaccharide molecules (Liu et al. 2010; Li and Yu. 2014; Wang et al. 2013). Consequently, the aggregates of these biomacromolecules may influence the aggregation process of CuO NPs in divalent electrolytes. Therefore, it is of significant interest to systematically study how the polysaccharides affect fundamental processes such as the aggregation of CuO NPs, both in the presence and absence of divalent electrolytes, which is imperative to elucidate the toxicity and risks of CuO NPs in natural environments.

The overall objective of this study is to systematically investigate the interaction between alginate with CuO NPs in monovalent and divalent electrolyte solutions. To this end, alginate (model polysaccharides) was comprehensively characterized, and the impacts on CuO NP aggregation were investigated in monovalent (Na^+) or divalent (Ca^{2+}) electrolyte solutions at varying concentrations. The aggregation kinetics of CuO NPs in the absence or presence of alginate was examined through dynamic light scattering (DLS) and zeta potential. Batch sorption experiments were conducted to measure both the equilibrium and kinetics of alginate sorption onto CuO NPs, and FTIR analysis was performed to elucidate the interactions between alginate and nano-CuO. Transmission electron microscopy (TEM) and scanning electron microscope (SEM) were used to delineate the mechanisms for CuO NP stabilization and destabilization under various conditions.

Materials and methods

Chemical reagents

The chemical reagents used in this study, including HCl, NaOH, $NaNO_3$, and $Ca(NO_3)_2$, were purchased from Aladdin Reagent (Shanghai, China) and at least p.a. grade. The chemical stock solutions were prepared separately by dissolving chemicals into Milli-Q water (18.2 MΩ cm^{-1}, Millipore) and filtered through 0.22 μm filters (Millipore). All samples, unless otherwise specified, were prepared at pH 6.8 (nearly neutral solution). The pH of all solutions was adjusted to 6.8 with 1 mmol L^{-1} NaOH or HCl, measured by a pH meter (Hitachi, Japan). Sodium alginate (lyophilized powder, >98 %) was obtained from Sigma-Aldrich (St. Louis, MO) and used as received (model polysaccharides). The molecular weight of alginate ranged from 12 to 80 kDa, with 61 % mannuronic acid and 39 % guluronic acid (Liu et al. 2010). The powder was analyzed by FTIR spectroscopy (Tensor 27, Bruker). To obtain the stock solutions, 200 mg powder sodium alginate was weighed into 500 mL Milli-Q water (18.2 MΩ cm^{-1}, Millipore) and stirred overnight to ensure total dissolution. Then, the alginate solution was filtered through a 0.22 μm cellulose membrane and kept in the dark at 4 °C. The total organic carbon content in the alginate stock solution was measured at 106.8 mg/L TOC (Liqui TOC II, Elementar, Germany).

Preparation of CuO NP dispersions

In this study, CuO nanopowder (vendor-reported size <100 nm) was purchased from Sigma-Aldrich (St. Louis, MO) (Table 1 for detailed properties). Stock suspension of CuO NPs was prepared by adding 0.5 g of CuO NPs to 1 L

of Milli-Q water. Then, the stock suspension was probe-sonicated in an ice-water bath to avoid uncontrolled heating at 25 °C. Firstly, the effects of ultrasonic time (5, 10, 15, 20, 25, and 30 min) and ultrasonic power (100, 200, 400, and 600 W) (ultrasonic cell crusher, Biosafer 1200-98) on the particle size distribution of CuO NPs were investigated in order to obtain the best dispersion procedure. Then, according to the optimal treatment, the stock suspension was prepared and the physicochemical properties of CuO NPs were characterized using dynamic light scattering (DLS) using Malvern Zetasizer (Nano ZSP, Malvern Instruments, UK) and UV-vis spectroscopy. The zeta potential of CuO NPs was measured in Milli-Q water over a wide range of pH values (5–10.5) at 25 °C. The concentration of the suspended nanoparticles used was adequate to create sufficient scattered intensity. The morphology and particle size of the CuO NPs in the stock suspension were characterized using a JEM-2100 transmission electron microscopy (TEM, JEOL Co., Japan).

Aggregation kinetics of CuO NPs

Time-resolved DLS (TR-DLS) measurements using a Malvern Zetasizer (Nano ZSP, Malvern Instruments, UK) were performed to study the increase of nano-CuO intensity-weighted averaged hydrodynamic diameter (HDD) with time (Shen et al. 2015). The detector employed a He-Ne laser at a wavelength of 633 nm and detection angle of 173° with each autocorrelation function being accumulated for 10 s. High polydispersity limits the reliability of nanoparticle HDD values (Kroll et al. 2014), and thus, data sets with a polydispersity index (PDI) above 0.7 were not taken into account. The measurements were conducted at 25 °C, and HCl and NaOH were used to adjust pH to 6.8.

The aggregation kinetics of CuO NPs was first tested in two electrolyte solutions (0–500 mM $NaNO_3$ and 0–50 mM $Ca(NO_3)_2$) without alginate addition. The effect of alginate on the aggregation of CuO NPs was investigated with aqueous alginate concentrations of 5 mg/L C (corresponding to typical freshwater natural organic matter concentration) (Loosli et al. 2015). In these experiments, a certain amount of electrolyte stock solution was added into the DLS cuvette which contained a predetermined volume of diluted nano-CuO stock solution and alginate so that the total volume of the final suspension was 1 mL. The concentration of CuO NPs in the DLS vial was maintained at 100 mg/L. Then, the tested suspensions were vortexed (WH-2, Huxi Analysis Instrument Factory, Shanghai) for 1 s immediately after mixing and then placed in the Zetasizer (Huangfu et al. 2013). At the initial stage of aggregation, the aggregation rate constant is directly proportional to the initial aggregation rate for Rh with time. Then, the particle attachment efficiency (α, i.e., inverse stability ratio, $1/W$) was evaluated, which was defined as the k normalized by the aggregation rate constant measured under a diffusion-limited (fast) regime (Chen et al. 2006; Shen et al. 2015). Details of the TR-DLS measurements, calculation methods for attachment efficiency (α), and critical coagulation concentration (CCC) are given in the supplementary material.

Zeta potential measurement

The electrophoretic mobility of CuO nanoparticles was evaluated by a Zetasizer (Nano ZSP, Malvern Instruments, UK) and converted to zeta potential using the Smoluchowski equation (Baalousha 2009). EPMs of CuO NPs in alginate-free electrolyte solutions were measured at a range of $NaNO_3$ and $Ca(NO_3)_2$ concentrations. Sample preparation was performed in the same way as the samples for the aggregation experiments. At least ten measurements were conducted for each sample employed. For measurements in the presence of polysaccharides, a concentration of 5 mg/L C alginate was employed. The measurements were taken at room temperature (25 °C), and all the experiments were run in duplicate or triplicate.

Spectroscopic analysis

TEM (JEM-2100), SEM (Hitachi S-4800), and energy-dispersive spectroscopy (EDS) analyzer were used to analyze the aggregates of the CuO NPs in the $Ca(NO_3)_2$ solution in the presence and absence of alginate. For the sample preparation, several drops of the CuO NP suspension were deposited onto a 300-mesh carbon-coated copper grid (Nanjing Zhongjing Technology Co., China) in a dust-free condition (Huangfu et al. 2013). The excess water was then removed with filter papers and the grid was air-dried for 30 min. Then, at least 20 representative images were taken for each sample. Simultaneously, EDS spectra were recorded at selected areas on the aggregate surface to obtain information on the surface atomic distribution and chemical composition.

Alginate-adsorbed nano-CuO powder was recovered by centrifuging the suspension and drying in a vacuum oven at 60 °C overnight. FTIR spectra of sample pellets with KBr were recorded on a Fourier transform infrared (FTIR) spectrometer (Tensor 27, Bruker). Infrared spectra of all nanoscale materials were collected from 4000 to 400 cm^{-1} range at room temperature (25 °C).

Results and discussion

Characterization of CuO NPs

Major physicochemical properties of CuO nanoparticles are summarized in Table 1. A TEM image of CuO NPs is provided

Table 1 Summary of CuO nanoparticle properties used in this study

Parameter	Value
Density (g/cm^3)	6.372
Vendor-reported size (nm)	60–100
TEM particle size measured (nm) ($n = 20$)	92 ± 12
DLS HDD measured in Milli-Q water (nm) ($n = 12$)	281 ± 27
BET specific surface area measured (m^2/g) ($n = 3$)	29 ± 3
Point of zero charge	8.8
Zeta potential (mV) in Milli-Q water (pH = 7)	+21.3 ± 1.6
Purity by ICP-MS (wt%)	98.81

The measured nano-CuO sizes showed significantly different between TEM and DLS measurements ($p < 0.05$). The purity of CuO NPs used in this study was determined through acid (HNO_3) digestion, and the concentrations of Cu^{2+} were analyzed by inductively coupled plasma mass spectrometry (ICP-MS, Agilent 7700×)

HDD hydrodynamic diameter

in Fig. S1, and the presence of CuO was evidenced by the FTIR spectra in Fig. S2 in the SI. The effects of ultrasonic time (5, 10, 15, 20, 25, and 30 min) and ultrasonic power (100, 200, 400, and 600 W) on the particle size distribution of CuO NP stock (500 mg/L) in Milli-Q water were investigated by DLS measurements. As shown in Figure S3(A), the dispersion stability of CuO NP suspension was jointly affected by both the sonication time and the ultrasonic power. The best dispersion procedure was obtained by 25-min sonication with ultrasonic power of 400 W, and no significant difference in aggregate size distributions was observed increasing the ultrasonic time over 25 min with ultrasonic power over 400 W.

According to the optimal treatment, the stock suspension was prepared after 30-min sonication with ultrasonic power of 600 W. CuO NPs in the stock suspension showed a positive charge with a zeta potential of +21.3 ± 1.6 mV. The intensity-weighted mean hydrodynamic diameter of CuO NPs in the stock suspension measured by DLS was 273 ± 37 nm (polydispersity index (PDI), 0.279) (Fig. S3(B)), indicating the majority were in well dispersion in Milli-Q water. Much larger size of CuO NPs measured by DLS compared to the primary size (60–100 nm) and the TEM measurements ($p < 0.05$) is likely due to the formation of nano-CuO aggregates, and the diameter measured by DLS is a value that refers to how a particle moves within a liquid (called the hydrodynamic diameter) (Majedi et al. 2014; Zhang et al. 2012). Zeta potential was measured at various pH values as shown in Fig. S4. The zeta potential is positive between pH 5 and 6 and is zero at pH 8.8, above which it becomes negative. These results are in good agreement with those reported by Sousa and Teixeira (2013), who have determined the point of zero charge for CuO NPs at pH ~9.

CuO NP aggregation kinetics with monovalent and divalent cations

The effects of monovalent and divalent cations on CuO NP aggregation were studied with 0–500 mM $NaNO_3$ and 0–20 mM $Ca(NO_3)_2$ (at pH 6.8). Representative aggregation profiles of CuO NPs obtained from TR-DLS measurements are presented in Figure S5. For the two electrolytes, the increase in electrolyte concentrations leads to a corresponding increase in the aggregation rate as a function of time up to a certain concentration above which the aggregation rate does not increase any further. These aggregation behaviors of CuO NPs in $NaNO_3$ and $Ca(NO_3)_2$ solution are consistent with the DLVO theory. The DLVO-type interactions were also discussed for NP aggregation kinetics (e.g., MnO_2 NPs and fullerenes (C_{60})) (Huangfu et al. 2013; Shen et al. 2015).

The zeta potentials (in mV) and representative α measured over a range of monovalent ($NaNO_3$) and divalent ($Ca(NO_3)_2$) electrolyte concentration (at pH 6.8) are presented in Fig. 1. CuO nanoparticles (with positive charge) exhibited a decrease in surface charge with increasing electrolyte concentration (Fig. 1a). It is proposed that $NaNO_3$ and $Ca(NO_3)_2$ ions could cover the nanoparticle surface and form an ion shield, which can promote nano-CuO aggregation (Khan et al. 2011; Shih et al. 2012). In addition, $Ca(NO_3)_2$ showed a higher efficiency in increasing zeta potential than the $NaNO_3$, and the zeta potential rapidly reduced from +21 to +2 mV when the concentration of $Ca(NO_3)_2$ was increased from 0 to 20 mM (Fig. 1a). Because NPs tend to aggregate when their surface charge is close to zero, the more significant influence of divalent counter-ions on CuO NP aggregation than the monovalent counter-ions was suggested through the changes of zeta potential (Son et al. 2015; Sousa and Teixeira 2013). The aggregation attachment efficiency (α) analysis of CuO NPs in the $NaNO_3$ and $Ca(NO_3)_2$ solutions clearly depicted a reaction-limited (slow) and diffusion-limited (fast) aggregation regime (Fig. 1b). The minimum electrolyte concentration required for fast aggregation was defined as critical coagulation concentration (CCC). In this study, extrapolation between the two regimes yielded CCC values of 54.5 and 2.9 mM for $NaNO_3$ and $Ca(NO_3)_2$, respectively, which were comparable with the reported results for CuO NPs in previous studies (Adeleye et al. 2014; Sousa and Teixeira 2013). Increasing the IS and divalent cation concentrations results in the compression of the electrostatic double layer because inter-particle repulsions diminish (Zhang et al. 2009). The same phenomena were also observed in the case of MnO_2 colloids (Huangfu et al. 2013) and Ag NPs (Khan et al. 2011).

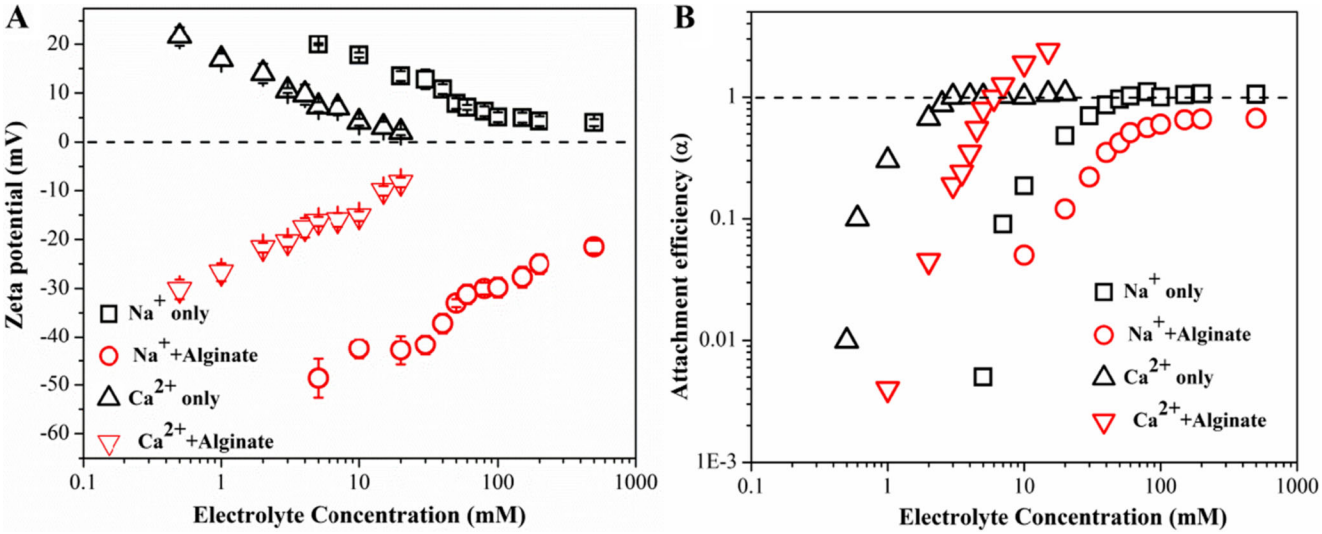

Fig. 1 **a** Zeta potential of CuO NPs as a function of $NaNO_3$ and $Ca(NO_3)_2$ concentration in the absence or presence of 5 mg/L C alginate; **b** aggregation attachment efficiencies of CuO NPs as a function of $NaNO_3$ and $Ca(NO_3)_2$ concentration in the absence or presence of 5 mg/L C alginate. Aggregation experiments and zeta potential measurements were conducted at pH 6.8 and 25 °C

Increased stability of CuO NPs with monovalent cations in the presence of alginate

The effects of alginate on the aggregation and stability of CuO NPs were investigated with a wide range of Na^+ and Ca^{2+} concentrations. As shown in Fig. 1, nano-CuO aggregation was significantly suppressed in the presence of alginate in Na^+ solution and similar results were also obtained in the case of TiO_2 NPs (Gallego-Urrea et al. 2014; Loosli et al. 2015) and hematite nanoparticles (Chen et al. 2006). Over the entire $NaNO_3$ concentration range, the values of nano-CuO attachment efficiency in the presence of alginate were lower than those in the absence of alginate (Fig. 1b), indicating that alginate enhanced the stability of CuO NPs. According to the results of zeta potential, the surface charge of CuO NPs changed from positive to negative on the addition of alginate for the $NaNO_3$ systems (Fig. 1a), which indicated that the negatively charged functional groups of alginate such as carboxylates were attached to the surface of the CuO NPs. These results suggested the relative importance of electrostatic repulsive interactions. Similar effect of alginate on particle charge was observed in the case of hematite as well (Chen et al. 2006). With the electrolyte concentration increasing, however, negative zeta potentials of alginate-coated nanoparticles decreased, since the charges would have been effectively screened by the high $NaNO_3$ concentration. The right shift of CCC and attenuation of α values strongly indicated that the steric hindrance combined with electrostatic effect was the predominant mechanism affecting the stability of CuO NPs in solutions of alginate/$NaNO_3$. Previously, the stabilizing effect of HA on magnetite nanoparticles was attributed to the combined electrostatic and steric effect (Illés and Tombácz 2006).

Enhanced aggregation of CuO NPs with divalent cations in the presence of alginate

Accordingly, the aggregation of CuO NPs in the presence of alginate and $Ca(NO_3)_2$ is different from that in the presence of alginate and $NaNO_3$. As shown in Fig. 1b, at low $Ca(NO_3)_2$ concentrations, the CuO NPs are more stable than in the presence of alginate, which can be explained by the steric influence imposed by the adsorbed alginate on the CuO NPs. It is widely reported that the stabilization of many particles was attributed to steric effects in the presence of alginate (Huangfu et al. 2013; Loosli et al. 2015). In addition, it is noteworthy that the adsorption quantity of alginate onto CuO NPs in the presence of $Ca(NO_3)_2$ was much higher than that in $NaNO_3$ solution (Figure S6); however, $Ca(NO_3)_2$ showed a higher efficiency in decreasing zeta potential than the $NaNO_3$ at the same molarity in the presence of alginate in this study (Fig. 1a). Although the adsorbed alginate would impart a negative charge onto the surface of CuO NPs, the interactions between Ca^{2+} cations and negative functional groups would impede the increase of zeta potential (Shen et al. 2015).

Nevertheless, as the Ca^{2+} concentration was increased, the co-presence of alginate and high Ca^{2+} concentration (>6 mM) resulted in significant increase in hydrodynamic diameter of CuO NPs (as shown in Fig. 2). Furthermore, there was a corresponding increase in the attachment efficiency to values above unity (Fig. 1b), indicating that the steric effects were not

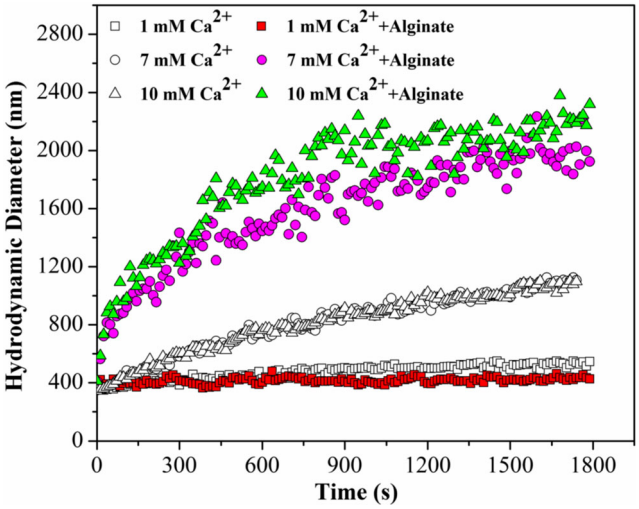

Fig. 2 Aggregation profiles of CuO NPs in various concentrations of $Ca(NO_3)_2$ solutions in the absence and presence of 5 mg/L C alginate at pH 6.8 and 25 °C

the predominant for the CuO NPs at high Ca^{2+} concentration (>6 mM) in the presence of alginate in this study. These observations strongly indicated that at high Ca^{2+} concentration, different aggregation mechanisms may be involved in the presence of alginate, which results in the enhanced aggregation kinetics, which will be studied next.

Alginate bridging leads to enhanced aggregation

TEM images of nano-CuO aggregates in the presence of Ca^{2+} and the co-presence of Ca^{2+} and alginate were captured to compare the morphology and to delineate the aggregation mechanisms (Shen et al. 2015). As shown in Fig. 3, in the absence of alginate, aggregates of CuO NPs can be observed where the particles are in close proximity to each other at 10 mM Ca^{2+}, at approximately 1 h after the initiation of nano-CuO aggregation. The aggregation is probably due to the decreasing surface charge of CuO NPs caused by the addition of $Ca(NO_3)_2$. However, in the presence of Ca^{2+} (10 mM) and alginate (5 mg/L C), it appears that CuO nanoparticles were embedded on the gel-bead structures formed by the clusters of alginate, and condensed shades of Ca^{2+}/alginate aggregates as bridges among nano-CuO particles in the TEM images were observed.

In addition, the bridging mechanism was further evidenced by elemental mapping obtained from SEM-EDS analysis. In copper mapping, the copper element positions were well consistent with the SEM image, with either absence or presence of alginate (Fig. 4). However, the presence of alginate resulted in an obvious decrease of the correspondence of the calcium elements with the nano-CuO aggregate positions when compared with that of aggregate in the absence of alginate (Fig. 4). This suggested that different mechanisms are predominant in the absence and presence of alginate. In the absence of alginate, CuO nanoparticles formed the aggregates via $Ca(NO_3)_2$ adsorption and the charge screening; thus, the mapping of calcium was in accordance with the area of the nano-CuO aggregate. In contrast, there was a wider distribution of the calcium element than the copper element in the presence of alginate, suggesting the Ca^{2+}/ alginate complex adsorbed on the surface of CuO NPs, which confirmed the bridging mechanism for CuO nanoparticles. In addition, calcium is known to bridge the molecules in the alginate network (β-D-mannuronate and α-L-guluronate) to form gel-like aggregates (Gallego-Urrea et al. 2014), which is also possible to see in the EDX mapping (Fig. 4), and will be discussed next.

Hetero-coagulation mechanism between CuO NPs and the unabsorbed alginate

Besides, as calculated from the adsorption tests, only about 20~35 % of alginate could be adsorbed onto 100 mg/L CuO NPs (Figure S6), leaving the majority of alginate in both the electrolyte solutions in this study. According to the literature, Ca^{2+} has the ability of producing aggregation of alginate molecules above a certain cation concentration due to the complexation of the carboxylic groups (Kloster and Avena 2015). Thus, the above quantitative comparison of the amounts of adsorbed alginate and the unadsorbed alginate allows us to hypothesize a hetero-coagulation mechanism between the alginate-covered CuO NPs and the unabsorbed alginate under high concentration of $Ca(NO_3)_2$ in this study.

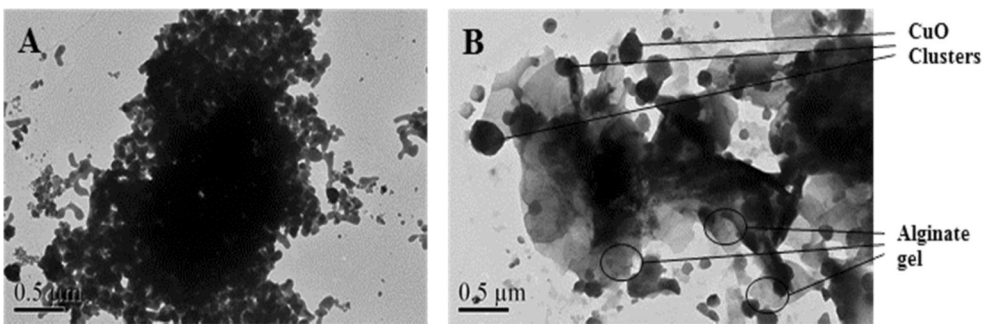

Fig. 3 Representative TEM images of CuO NPs in the presence of **a** Ca^{2+} and **b** Ca^{2+} and alginate (Ca^{2+} = 10 mM; alginate = 5 mg/L C). TEM images were captured from samples collected 1 h after the initiation of aggregation

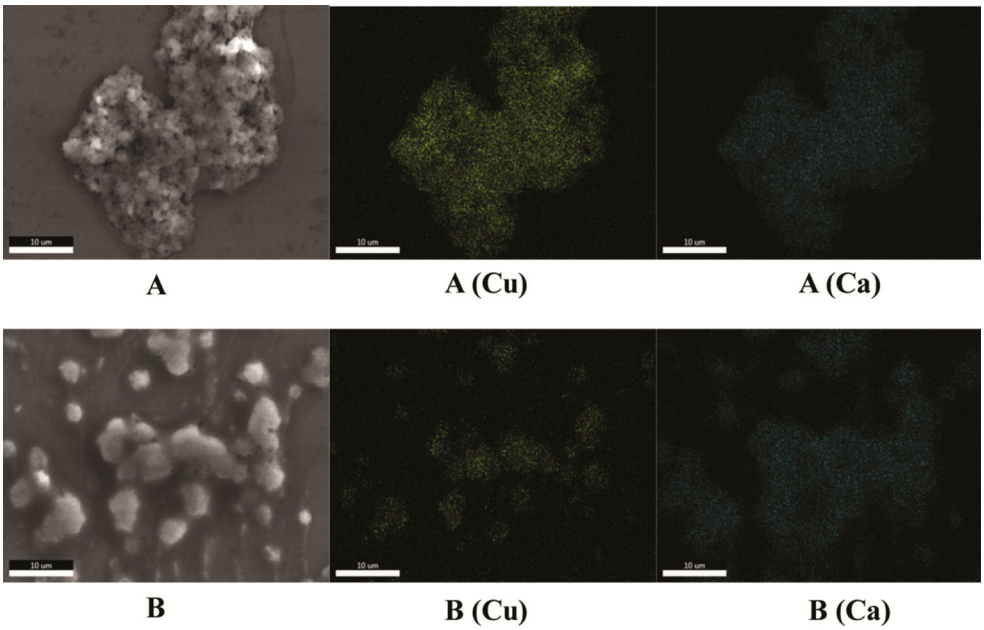

Fig. 4 Representative SEM-EDS images with element mapping of CuO NPs in the presence of **a** Ca^{2+} and **b** Ca^{2+} and alginate (Ca^{2+} = 10 mM; alginate = 5 mg/L C). SEM images were captured from samples collected 1 h after the initiation of aggregation

To further investigate the role of Ca^{2+}-induced alginate aggregation in the $Ca(NO_3)_2$ systems, the scattered light intensities from separately prepared alginate solutions with different electrolytes were measured with respect to time by employing the light scattering setup following the method described by Chen and Elimelech (2007). The alginate solutions were prepared at the same concentration as the DLS experiments of 5 mg/L TOC at pH 6.8, and the aggregation experiments of alginate were conducted following the procedures described in section "Aggregation kinetics of CuO NPs."

Figure S7 shows the scattered light intensities from the alginate solutions normalized by the incident laser intensity in the presence of the $NaNO_3$ and $Ca(NO_3)_2$ electrolytes. At high Na^+ concentrations (200 mM), the normalized scattered light intensities remained constant at slightly higher values than that of water, suggesting that the relatively dilute alginate solutions did not form aggregates. In contrast, in the presence of 10 mM Ca^{2+}, the normalized scattered light intensity increases with time, indicating significant aggregation of alginate macromolecules. Then, the concentration of alginate was increased to 25 mg TOC, in order to observe the aggregation of alginate in the $NaNO_3$ and $Ca(NO_3)_2$ electrolytes. Over the entire $NaNO_3$ concentration range, $<D_h>$ remained about 100 nm, indicating the stability of alginate colloids (data not shown). In contrast, as the Ca^{2+} concentration increased from 1 to 4.5 mM, the $<D_h>$ exhibited a slightly increase (below 400 nm), while a rapid rise of $<D_h>$ was observed when the

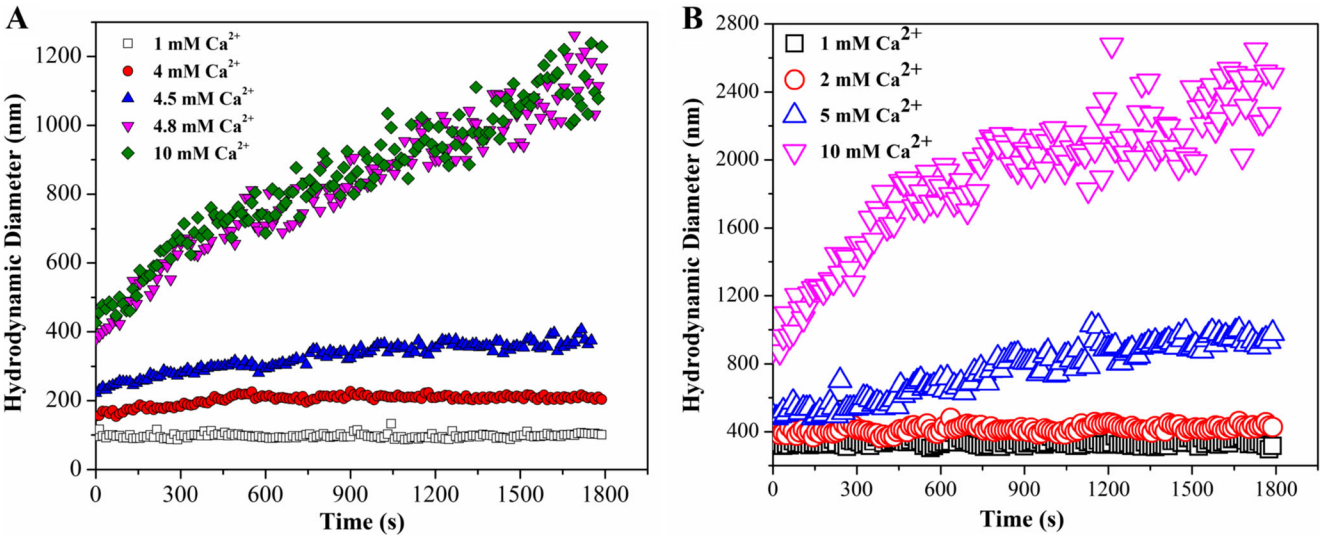

Fig. 5 **a** Aggregation profiles of alginate (25 mg/L C) in various concentrations of $Ca(NO_3)_2$ solutions at pH 6.8 and 25 °C. **b** Aggregation profiles of CuO NPs in the presence of alginate (25 mg/L C) in various concentrations of $Ca(NO_3)_2$ solutions at pH 6.8 and 25 °C

$Ca(NO_3)_2$ concentration exceeded 4.8 mM (Fig. 5a). Bound divalent cations could form intra- and/or intermolecular bridges between adjacent alginate colloids, and as a result increase the attractive intermolecular forces (Wang et al. 2013). Thus, divalent Ca^{2+} is considered to rapidly interact with alginate molecules, and the combined effects of charge screening, calcium complexation as well as bridging lead to the rapid formation and growth in the size of the alginate aggregates.

Based on the above observations and discussion, another experimental group was conducted, in which the aggregation kinetics of CuO NPs (100 mg/L) was determined with the presence of alginate (25 mg/L TOC) in various concentrations of $Ca(NO_3)_2$ solutions at pH 6.8 and 25 °C. The measured $<D_h>$ of the aggregates in the solution increased significantly with the increasing of Ca^{2+} concentrations (Fig. 5b), consistent with the results obtained from the alginate aggregation. The results may indicate hetero-aggregation of alginate molecules and CuO NPs in solution of high concentration of Ca^{2+}. Although it is very difficult to discriminate between Ca^{2+}-induced aggregation of alginate molecules and direct aggregation of nano-CuO/alginate complex, it is possible to infer that hetero-aggregation would be the prevailing process when the NPs were released into the aqueous systems enriched with NOM. Thus, further studies should be conducted to investigate the NP stability under more complex and environmentally relevant conditions in the future.

Conclusion and implications

This study provides an insight into the stability of CuO nanoparticles in various ionic strength conditions with and without the presence of alginate. It appears that, in the absence of alginate, significant aggregation of CuO NPs was observed in the two electrolyte solutions ($NaNO_3$ and $Ca(NO_3)_2$), especially for $Ca(NO_3)_2$. The presence of alginate had pronounced effects on the particle size distribution of CuO NPs and greatly enhanced the aggregation of CuO NPs in high concentration of Ca^{2+} solutions, confirmed by DLS measurements. The morphology of the aggregates of CuO NPs formed under different solutions was observed by TEM analysis. Besides, significant coagulation of the alginate molecules was observed in solutions of high Ca^{2+} concentrations, suggesting a hetero-coagulation mechanism between the alginate-covered CuO NPs and the unabsorbed alginate under high concentration of $Ca(NO_3)_2$. The results presented in this study suggested that not only the presence of NOM but also the ratio between NP and NOM should be taken into consideration in studying the NP stability in aqueous systems, due to the interaction between the multivalent cations and the ubiquitous organic matter (Kloster et al. 2013; Wang et al. 2013). More studies should be conducted to extend to more complex and environmentally relevant conditions in the future. Thus, specific conditions in aquatic environments play a very important role in evaluating the fate and transport of engineered nanoparticles, which ultimately have impacts on uptake and therefore bioavailability and toxicity of ENPs to aquatic organisms.

Acknowledgments We are grateful for the grants from the project supported by the National Science Funds for Creative Research Groups of China (No. 51421006), the National Science Funds for Distinguished Young Scholars (No. 51225901), the National Natural Science Foundation of China (No. 41430751, 51479047, 51479065), the Program for Changjiang Scholars and Innovative Research Team in University (No. IRT13061), the National Science Foundation of China for Excellent Young Scholars (No. 51422902), the Fundamental Research Funds for the Central Universities (No. 2015B22014, No. 2015B05714), and PAPD.

References

Adeleye AS, Conway JR, Perez T, Rutten P, Keller AA (2014) Influence of extracellular polymeric substances on the long-term fate, dissolution, and speciation of copper-based nanoparticles. Environ Sci Technol 48:12561–12568

Aiken GR, Hsu-Kim H, Ryan JN (2011) Influence of dissolved organic matter on the environmental fate of metals, nanoparticles, and colloids. Environ Sci Technol 45:3196–3201

Applerot G, Lellouche J, Lipovsky A, Nitzan Y, Lubart R, Gedanken A, Banin E (2012) Understanding the antibacterial mechanism of CuO nanoparticles: revealing the route of induced oxidative stress. Small 8:3326–3337

Aruoja V, Dubourguier HC, Kasemets K, Kahru A (2009) Toxicity of nanoparticles of CuO, ZnO and TiO_2 to microalgae *Pseudokirchneriella subcapitata*. Sci Total Environ 407(4): 1461–1468

Baalousha M (2009) Aggregation and disaggregation of iron oxide nanoparticles: influence of particle concentration, pH and natural organic matter. Sci Total Environ 407(6):2093–2101

Burkart C, von Tümpling W, Berendonk T, Jungmann D (2015) Nanoparticles in wastewater treatment plants: a novel acute toxicity test for ciliates and its implementation in risk assessment. Environ Sci Pollut R 22(10):7485–7494

Chang YN, Zhang M, Xia L, Zhang J, Xing G (2012) The toxic effects and mechanisms of CuO and ZnO nanoparticles. Materials 5: 2850–2871

Chen KL, Elimelech M (2007) Influence of humic acid on the aggregation kinetics of fullerene (C60) nanoparticles in monovalent and divalent electrolyte solutions. J Colloid Interface Sci 309(1): 126–134

Chen KL, Mylon SE, Elimelech M (2006) Aggregation kinetics of alginate-coated hematite nanoparticles in monovalent and divalent electrolytes. Environ Sci Technol 40:1516–1523

Gallego-Urrea JA, Holmberg JP, Hassellöv M (2014) Influence of different types of natural organic matter on titania nanoparticle stability: effects of counter ion concentration and pH. Environ Sci: Nano 1(2): 181–189

Grillo R, Rosa AH, Fraceto LF (2015) Engineered nanoparticles and organic matter: a review of the state-of-the-art. Chemosphere 119: 608–619

Hou J, Miao L, Wang C, Wang P, Ao Y, Lv B (2015) Effect of CuO nanoparticles on the production and composition of extracellular polymeric substances and physicochemical stability of activated sludge flocs. Bioresour Technol 176:65–70

Huangfu X, Jiang J, Ma J, Liu Y, Yang J (2013) Aggregation kinetics of manganese dioxide colloids in aqueous solution: influence of humic substances and biomacromolecules. Environ Sci Technol 47:10285–10292

Illés E, Tombácz E (2006) The effect of humic acid adsorption on pH-dependent surface charging and aggregation of magnetite nanoparticles. J Colloid Interface Sci 295(1):115–123

Karlsson HL, Cronholm P, Gustafsson J, Moller L (2008) Copper oxide nanoparticles are highly toxic: a comparison between metal oxide nanoparticles and carbon nanotubes. Chem Res Toxicol 21: 1726–1732

Khan SS, Mukherjee A, Chandrasekaran N (2011) Impact of exopolysaccharides on the stability of silver nanoparticles in water. Water Res 45(16):5184–5190

Kloster N, Avena M (2015) Interaction of humic acids with soil minerals: adsorption and surface aggregation induced by Ca^{2+}. Environ Chem. http://dx.doi.org/10.1071/EN14157

Kloster N, Brigante M, Zanini G, Avena M (2013) Aggregation kinetics of humic acids in the presence of calcium ions. Colloid Surface A 427:76–82

Kroll A, Behra R, Kaegi R, Sigg L (2014) Extracellular polymeric substances (EPS) of freshwater biofilms stabilize and modify CeO_2 and Ag nanoparticles. PLoS One 9, e110709

Li WW, Yu HQ (2014) Insight into the roles of microbial extracellular polymer substances in metal biosorption. Bioresour Technol 160: 15–23

Liu X, Wazne M, Han Y, Christodoulatos C, Jasinkiewicz KL (2010) Effects of natural organic matter on aggregation kinetics of boron nanoparticles in monovalent and divalent electrolytes. J Colloid Interface Sci 348(1):101–107

Loosli F, Le Coustumer P, Stoll S (2015) Effect of electrolyte valency, alginate concentration and pH on engineered TiO_2 nanoparticle stability in aqueous solution. Sci Total Environ 535:28–34

Majedi SM, Kelly BC, Lee HK (2014) Role of combinatorial environmental factors in the behavior and fate of ZnO nanoparticles in aqueous systems: a multiparametric analysis. J Hazard Mater 264: 370–379

Miao L, Wang C, Hou J, Wang P, Ao Y, Dai S, Lv B (2014) Effects of pH and natural organic matter (NOM) on the adsorptive removal of CuO nanoparticles by periphyton. Environ Sci Pollut R 22(10): 7696–7704

Nowack B, Bucheli TD (2007) Occurrence, behavior and effects of nanoparticles in the environment. Environ Pollut 150:5–22

Nowack B, Ranville JF, Diamond S, Gallego-Urrea JA, Metcalfe C, Rose J, Klaine SJ (2012) Potential scenarios for nanomaterial release and subsequent alteration in the environment. Environ Toxicol Chem 31(1):50–59

Philippe A, Schaumann GE (2014) Interactions of dissolved organic matter with natural and engineered inorganic colloids: a review. Environ Sci Technol 48:8946–8962

Shen MH, Yin YG, Booth A, Liu JF (2015) Effects of molecular weight-dependent physicochemical heterogeneity of natural organic matter on the aggregation of fullerene nanoparticles in mono-and di-valent electrolyte solutions. Water Res 71:11–20

Shih YH, Zhuang CM, Tso CP, Lin CH (2012) The effect of electrolytes on the aggregation kinetics of titanium dioxide nanoparticle aggregates. J Nanopart Res 14(8):1–11

Son J, Vavra J, Forbes VE (2015) Effects of water quality parameters on agglomeration and dissolution of copper oxide nanoparticles (CuO-NPs) using a central composite circumscribed design. Sci Total Environ 521:183–190

Sousa VS, Teixeira MR (2013) Aggregation kinetics and surface charge of CuO nanoparticles: the influence of pH, ionic strength and humic acids. Environ Chem 10(4):313–322

Wang LF, Wang LL, Ye XD, Li WW, Ren XM, Sheng GP, Wang XK (2013) Coagulation kinetics of humic aggregates in mono-and di-valent electrolyte solutions. Environ Sci Technol 47(10):5042–5049

Wilkinson KJ, Joz-Roland A, Buffle J (1997) Different roles of pedogenic fulvic acids and aquagenic biopolymers on colloid aggregation and stability in freshwaters. Limnol Oceanogr 42(8):1714–1724

Yang Y, Zhang C, Hu Z (2013) Impact of metallic and metal oxide nanoparticles on wastewater treatment and anaerobic digestion. Environ Sci Process Impacts 15:39–48

Zhang Y, Chen Y, Westerhoff P, Crittenden J (2009) Impact of natural organic matter and divalent cations on the stability of aqueous nanoparticles. Water Res 43:4249–4257

Zhang HY, Smith JA, Oyanedel-Craver V (2012) The effect of natural water conditions on the anti-bacterial performance and stability of silver nanoparticles capped with different polymers. Water Res 46: 691–699

Zhao J, Wang Z, Dai Y, Xing B (2013) Mitigation of CuO nanoparticle-induced bacterial membrane damage by dissolved organic matter. Water Res 47:4169–4178

Zhou K, Wang R, Xu B, Li Y (2006) Synthesis, characterization and catalytic properties of CuO nanocrystals with various shapes. Nanotechnology 17:3939

Zhou XH, Huang BC, Zhou T, Liu YC, Shi HC (2015) Aggregation behavior of engineered nanoparticles and their impact on activated sludge in wastewater treatment. Chemosphere 119:568–576